



Structure and magnetic ordering in the defect compound $\text{ErGe}_{1.83}$

O. Oleksyn^{1,a}, P. Schobinger-Papamantellos^{a,*}, C. Ritter^b, C.H. de Groot^c, K.H.J. Buschow^c

^aLaboratorium für Kristallographie, ETHZ, CH-8092 Zürich, Switzerland

^bInstitut Laue-Langevin, 156X, 38042 Grenoble Cédex, France

^cVan der Waals-Zeeman Institute, University of Amsterdam, 1018 XE Amsterdam, The Netherlands

Received 2 September 1996

Abstract

The crystal structure and the magnetic ordering of the novel orthorhombic compound ErGe_{2-x} has been studied by neutron powder diffraction and magnetic measurements. The crystal structure belongs to the $\text{DyGe}_{1.85}$ -type (space group $\text{Cmc}2_1$). ErGe_{2-x} ($x=0.17(2)$) orders antiferromagnetically below $T_N=6$ K with a uniaxial magnetic moment arrangement. The magnetic cell has the same size as the chemical unit cell ($\mathbf{q}=0$). The magnetic space group is $\text{Cmc}2_1$ (Sh_{36}^{173}). At $T=1.5$ K the magnetic moments of the two erbium sites have the same ordered magnetic moment value of $7.63(6) \mu_B/\text{Er}$ and are coupled antiferromagnetically along the a direction.

1. Introduction

The germanium/silicon rich concentration range (65–75% Ge/Si) of the (T, x) phase diagrams of the erbium germanium/silicon systems [1] comprise a large variety of phases that are presently studied by many investigators [2,3] because of their interesting electric and magnetic properties in view of potential applications in microelectronics. Several of these phases display homogeneity regions and give rise to polymorphic transformations as a function of temperature and composition. In this respect the compound ErGe_2 is of particular interest as it is reported to undergo two polymorphic transformations at 1080 K and 1205 K. The crystal structure of all modifications is unknown. The present investigation deals with the determination of the crystal structure and magnetic properties of the low temperature modification of the ErGe_2 phase.

2. Sample preparation and differential thermal analysis (DTA)

A polycrystalline sample of the nominal composition ErGe_2 was prepared by arc melting in a purified argon

atmosphere. The purity of the starting materials was 99.9% for Er and 99.99% for Ge, the weight loss after melting was less than 2 wt%. The ingot was annealed in vacuum at 1070 K for three weeks and then quenched to room temperature. The purity of the sample was examined by X-ray powder diffraction.

The thermal analysis was performed on a powdered and finely packed sample, under argon atmosphere in an alumina crucible using a Perkin-Elmer thermal analysis system. Two thermal effects were observed upon heating, while during cooling only one effect was visible (Fig. 1). The broadness of the peaks in the DTA trace does not allow us to define the transformation temperatures precisely. The values estimated by us are 1165 K and 1220 K, differing from those reported in [1]. The powder when heated up to 1273 K did not give any indication of melting.

3. Magnetic measurements

Magnetic measurements were made with a SQUID magnetometer. The high temperature data (50–300 K) show Curie Weiss behaviour (see Fig. 2a) with $\mu_{\text{eff}}=10.3 \mu_B/\text{Er}$ and a Curie Weiss intercept of $\Theta_p=8$ K. The temperature dependence of the magnetisation measured in a field of 0.1 T (see Fig. 2b) shows that ErGe_2 orders antiferromagnetically at about $T_N=6$ K.

The field dependence of the magnetisation at 5 K is displayed in Fig. 2c. These data confirm the antiferro-

*Corresponding author.

¹On leave from Institute of Inorganic Chemistry, Lviv State University, Lviv, Ukraine.

magnetic nature of ErGe_2 . There is a metamagnetic transition at about 0.5 T. In the regime of parallel Er moments observed in the highest field strength considered the moment value is seen to be approximately equal to the free ion value $9 \mu_B/\text{Er}$ atom.

4. Neutron diffraction

Neutron diffraction experiments were carried out at the facilities of the ILL reactor (Grenoble). The data at 1.5 and 80 K were collected on the D2B diffractometer $\lambda=1.549 \text{ \AA}$. The step increment in 2θ was 0.05° . The data analysis was performed by the Fullprof program [4].

4.1. Crystal structure

The 80 K data collected well above the Néel temperature (paramagnetic state) are displayed in Fig. 3(top part). The diffraction pattern was indexed by using the CSD [5] package in the C-centred orthorhombic lattice with unit cell constants $a \approx 4.05$, $b \approx 29.49$, $c \approx 3.88 \text{ \AA}$. Three distinct structural models although with similar unit cell dimensions and composition are known in the literature for the compounds $\text{DyGe}_{1.85}$ [6], $\text{DyGe}_{1.9}$ [7], $\text{Sm}_4\text{Co}_{1-x}\text{Ge}_7$ [8]. Satisfactory agreement between the experimental and calculated profiles was obtained only for the model with the atomic arrangement of the $\text{DyGe}_{1.85}$ structure type. As pointed out in the X-ray single crystal analysis [6] of the $\text{DyGe}_{1.85}$ compound the observed reflection conditions are compatible with two space groups: $Cmcm$ and $Cmc2_1$ which differ in the presence of a centre of symmetry, the main difference being the atomic surrounding of the Ge4

site. Even the use of the present high resolution neutron powder data of the D2B instrument and the comparable absolute values of the neutron coherent scattering length for Er and Ge atoms did not allow us to clarify the existence of a centre of symmetry. The refinement converged for both models: $R_n=5.9\%$ and $R_{wp}=15.6\%$, $R_{exp}=12.6\%$, $\chi^2=1.55$ for $Cmcm$ and $R_n=5.8\%$ and $R_{wp}=15.8\%$, $R_{exp}=12.5\%$, $\chi^2=1.61$ for $Cmc2_1$ (Table 1a). On the other hand, a physically more reasonable model is in favour of the noncentrosymmetric $Cmc2_1$ group. The action of the plane m_z is associated with a doubling of the multiplicity of the Ge4 site 4(a) in $Cmc2_1$ leading, to the 8(f) site in $Cmcm$. As can be seen in Fig. 4 this results in non realistic interatomic distances $\delta=0.732(8) \text{ \AA}$ between the Ge4 atoms in the latter model. The profile fit shown in Fig. 3 is based on the $Cmc2_1$ space group.

4.2. Magnetic structure

The data obtained in the magnetically ordered state at $T=1.5 \text{ K}$ were indexed with the same C-centred unit cell as found for the nuclear reflections ($\mathbf{q}=0$). There are four magnetic space groups associated with the magnetic C lattice and this wave vector [9,10]. All of them except the trivial one would allow ferromagnetic modes. The possible magnetic modes are given in Table 2. Two independent Er atoms occupy the 4(a) special Wyckoff position located in the mirror plane m_x . The refinement of magnetic intensities showed that the Er magnetic moments (see Fig. 5) are oriented along the a axis and that the atoms (1) $(0,y,z)$ and (2) $(0,-y,1/2+z)$ related by the screw operation 2_{1z} have opposite signs (the magnetic form factor used for Er^{3+} is from [11]). This arrangement remains invariant under the assumption of the trivial magnetic space group $Cmc2_1$ (Sh_{36}^{173}). The good agreement between the experimental and the calculated pattern (Fig. 3) and the low values of the reliability factors $R_n=3.8\%$, $R_m=7.3\%$, $R_{wp}=18.2\%$, $R_{exp}=13.0\%$, $\chi^2=1.96$ (Table 1) can be taken as evidence for the correctness of the magnetic model proposed. The ordered moment value $7.63(1) \mu_B/\text{Er}$ at 1.5 K is lower than the free-ion value of Er^{3+} and ($gJ\mu_B=9\mu_B$). The Er atoms related by the screw axis 2_1 operation and neighbouring Er atoms occupying different symmetry sites have their moments oppositely aligned. This gives rise to the uniaxial antiferromagnetic structure shown in Fig. 5. The interlayer interaction for both Er sublattices for layers at $z=1/4$ or $3/4$ is ferromagnetic while the intralayer interaction is antiferromagnetic.

5. Concluding remarks

We have confirmed the existence of a compound close to a 1:2 ratio in the ErGe system. The composition determined by diffraction methods is ErGe_{2-x} ($x=$

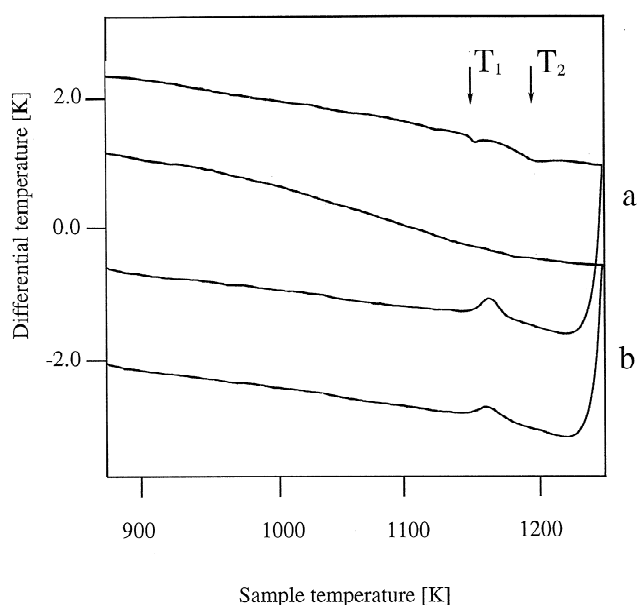


Fig. 1. Results of differential thermal analysis: heating (a) and cooling (b) curves. Transition points are marked by arrow $T_1=1165 \text{ K}$, $T_2=1220 \text{ K}$.

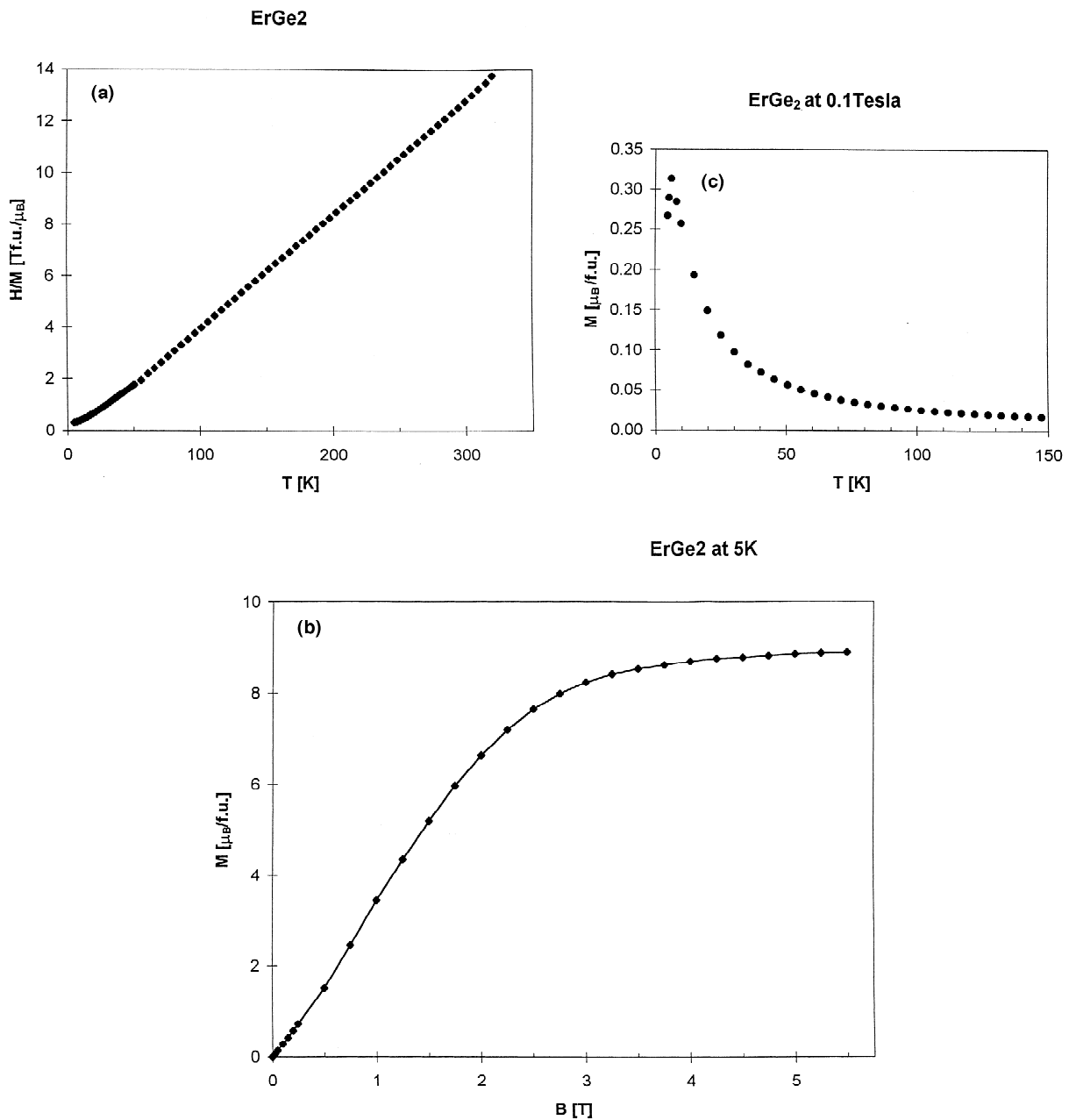


Fig. 2. (a) Temperature dependence of the reciprocal susceptibility of a sample of the nominal composition ErGe₂ measured in a field of 1 T. (b) Temperature dependence of the magnetisation measured in 0.1 T. (c) Field dependence of the magnetisation at 5 K.

0.17(2)). The existence of thermal effects in the DTA traces is in agreement with the fact that three polymorphic modifications occur, but the transformation temperature values obtained by us differ from those reported in [1].

The investigated crystal structure adds a further representative to the large family of nonstoichiometric RX_{2-x} compounds (R =rare-earth, X =Si, Ge) known to occur for a variety of distinct structures.

A common feature of the mentioned structures is a stacking of paired layers built of triangular prisms and tetragonal antiprisms. This feature is present also in the crystal structure of ErGe_{1.83} as determined in the course of

the present investigation. Alternatively the structure can be described as a linear combination of intergrown fragments of the AlB₂ and the ZrSi₂ structure types (Fig. 6). Three bands of (Er₆) trigonal prisms with X-atoms in the centre with parallel alignment of their axes alternate with columns of empty tetragonal antiprisms (Er₄Ge₄). Interatomic distances are strongly dependent on the size of the rare earth atoms and in ErGe_{1.83} (Table 3) they are indicative of covalent Ge–Ge bonding. Shortening of the distances between the Ge₄–Ge₄ atoms (2.04(1) Å) relative to the covalent bond length (2.44 Å) causes a partial occupation of this position.

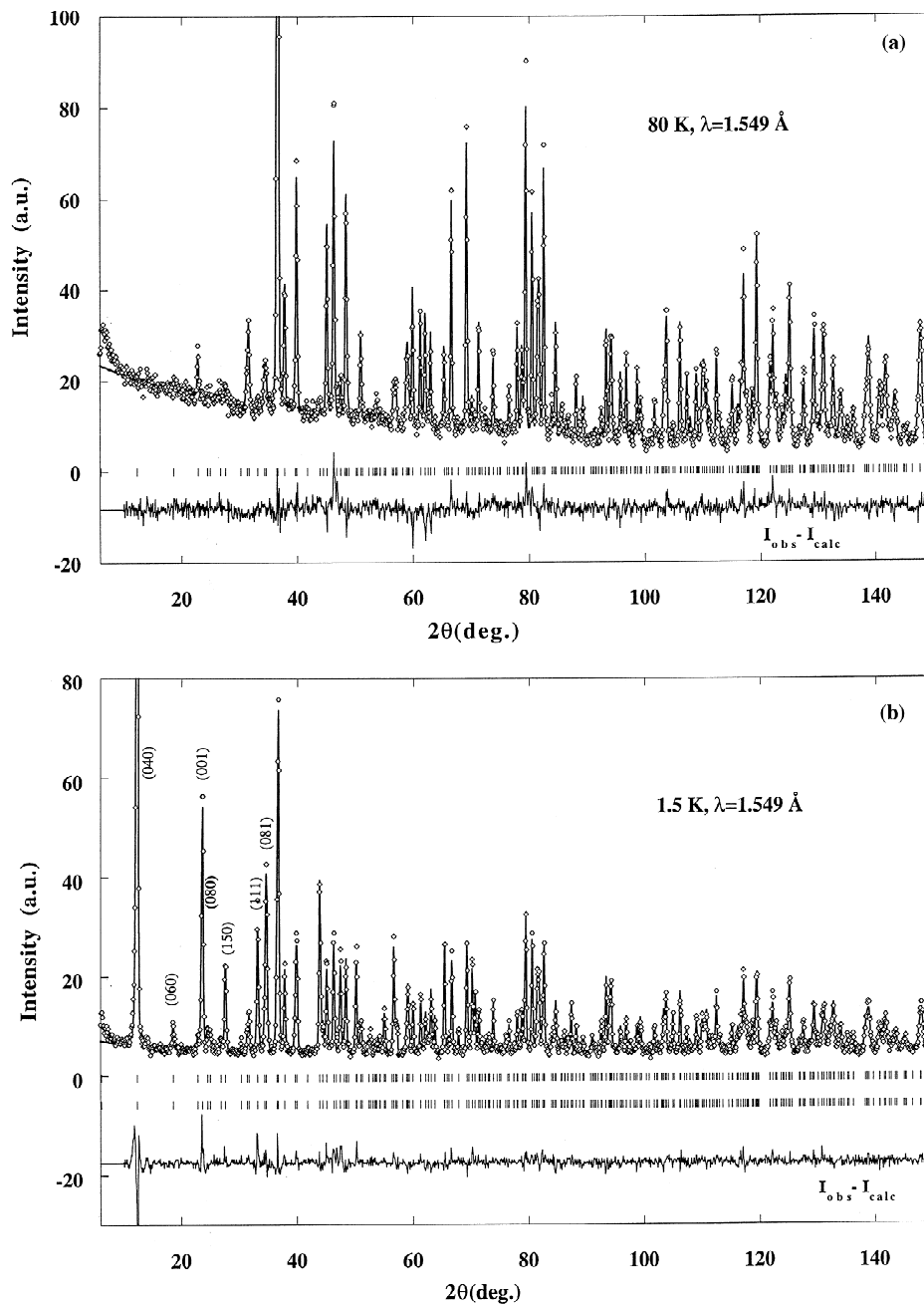


Fig. 3. Observed, calculated and difference neutron diagrams of $\text{ErGe}_{1.83}$ germanide: (a, top part) measured at 80 K (paramagnetic state); (b, bottom part) measured at 1.5 K (magnetically ordered state).

The magnetic structure found at 1.5 K corresponds to a uniaxial antiferromagnetic arrangement of the Er moments along the a -direction. The thermodynamically most stable ordering in TbGe_2 [12], $\text{DyGe}_{1.9}$ [7] is given by an alternating $+ - + -$ stacking of ferromagnetic layers along the longest orthorhombic axis b . The ferromagnetic intralayer interaction is retained also in $\text{ErGe}_{1.83}$. However, the antiferromagnetic interlayer interaction along the b direction has become substantially weakened because our

magnetic measurements have shown that the antiferromagnetic structure can be broken already in comparatively small external magnetic fields.

Finally we note that when the magnetic sublattice is more diluted by the nonmagnetic component (in the case of RGe_3 phases— TbGe_3 [13], DyGe_3 [14], ErGe_3 [15]) a more complex situation is found to occur which manifests itself by the presence of more than one wave vector and phase transition including incommensurate regions.

Table 1
Refined parameters from neutron data of $\text{ErGe}_{1.83}$ (space group $Cmc2_1$). All atoms occupy 4(a) sites with coordinates (0,y,z). For defining the origin the Er1 atom is fixed at $z=0.750$. The data refer to results obtained (a) at 80 K in the paramagnetic state, (b) at 1.5 K in the magnetically ordered state magnetic space group $Cmc2_1 (Sh_{36}^{173})$.

Temperature	80 K			1.5 K		
Atom	y	z	$B_{\text{iso}} 10^2 (\text{\AA})^2$	y	z	$B_{\text{iso}} 10^2 (\text{\AA})^2$
Er1	0.0603(1)	0.750	0.32(6)	0.0609(1)	0.750	0.32(9)
Er2	0.1726(1)	0.245(3)	0.16(5)	0.1710(1)	0.249(4)	0.16(8)
Ge1	0.3521(1)	0.248(3)	0.64(4)	0.3529(2)	0.268(4)	0.6(1)
Ge2	0.4078(1)	0.742(3)	0.72(4)	0.4074(2)	0.744(4)	0.72(9)
Ge3	0.2515(1)	0.742(3)	0.54(5)	0.2499(2)	0.765(4)	0.54(9)
Ge4	0.5104(1)	0.337(3)	1.7(2)	0.5101(5)	0.347(4)	1.7(3)
occup. Ge4	0.67(2)			0.64(2)		
$\mu_{\text{Er}} [\mu_B]$	-	-	-	7.63(6)		
$a(\text{\AA}), b(\text{\AA}), c(\text{\AA})$	4.05263(7)	29.4964(5)	3.88712(6)	4.05234(7)	29.4850(8)	3.88456(9)
$R_w\%, R_m\%$	5.78, -			3.80, 7.26		
$R_{\text{wp}}\%, R_{\text{exp}}\%, \chi^2$	15.8, 12.5, 1.61			18.2, 13.0, 1.96		

Table 2
The magnetic space groups of $Cmc2_1$ associated with the magnetic C lattice and $\mathbf{q}=0$.

Magnetic space group	x	y	z
$Cmc2_1 (Sh_{36}^{173})$	G_x	-	-
$Cm'c2_1' (Sh_{36}^{174})$	-	F_y	G_z
$Cmc'2_1' (Sh_{36}^{175})$	F_x	-	-
$Cm'c'2_1 (Sh_{36}^{176})$	-	G_y	F_z

The magnetic modes $F(++++)$ and $G(+--+)$ are of the 4(a) site. The signs refer to the atoms (1) (0,y,z); (2) (0,-y,z+1/2); (3) (1/2,y+1/2,z+1/2); (4) (1/2,-y+1/2,z+1/2).

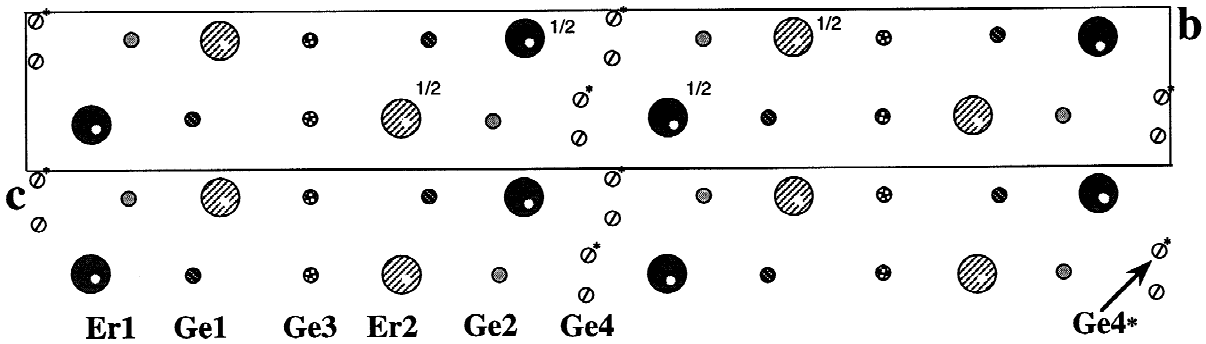


Fig. 4. The unit cell projection of $\text{ErGe}_{1.83}$ structure at (0,y,z) plane. In the $Cmcm$ space group germanium atoms occupy positions marked as Ge4 and Ge4*.

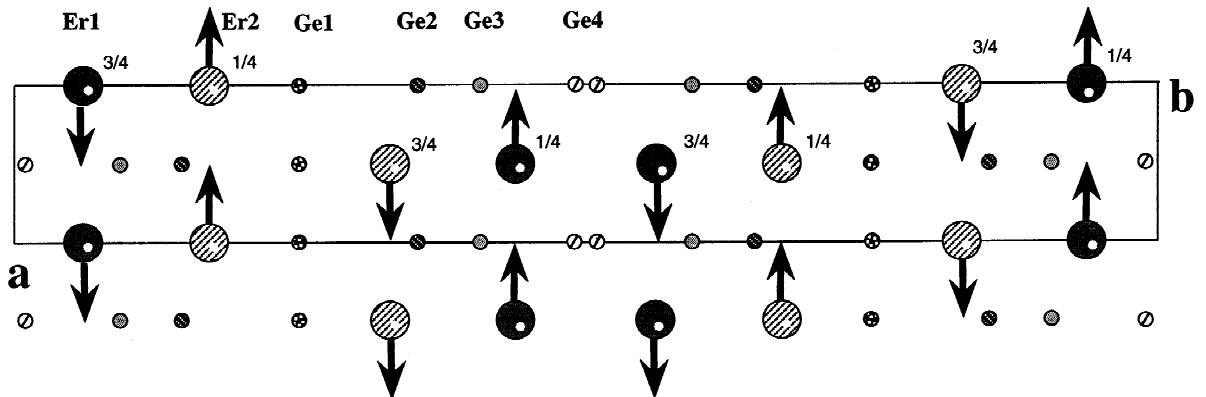


Fig. 5. Schematic representation of the collinear antiferromagnetic ordering in $\text{ErGe}_{1.83}$ when viewed along the [001] direction.

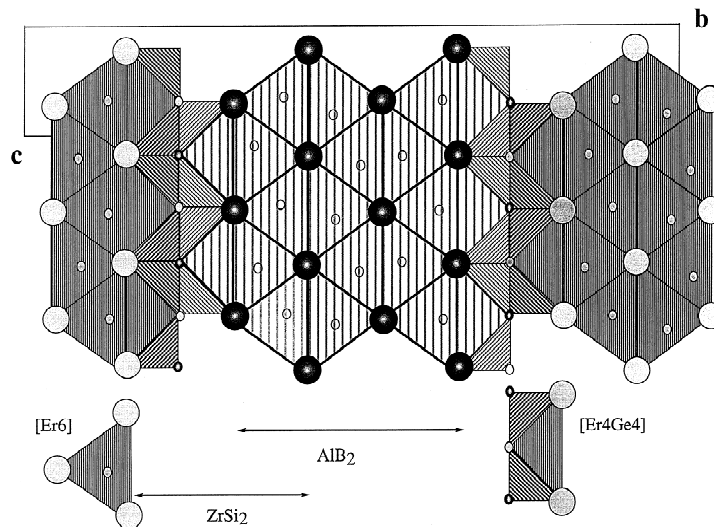


Fig. 6. Alternating stacking along the b axis of triangular $[Er_6]$ prisms and tetragonal $[Er_4Ge_4]$ antiprisms in $ErGe_{1.83}$ structure. The fragments of AlB_2 and $ZrSi_2$ structures types are extracted.

Table 3

The interatomic distances (\AA) between neighbouring atoms in the $ErGe_{1.83}$ structure (space group $Cmc2_1$).

Atoms	Distances	Atoms	Distances	Atoms	Distances
Er_1-2Ge_4	2.927(7)	Er_1-2Ge_1	3.283(3)	Er_1-2Er_1	3.89(6)
$-2Ge_2$	2.94(3)	$-2Ge_4$	3.39(3)	$-2Er_1$	4.0526(1)
$-2Ge_4$	2.97(2)	$-1Er_2$	3.83(2)	$-2Er_1$	4.0537(1)
$-2Ge_2$	2.98(3)	$-1Er_2$	3.85(2)		
Er_2-2Ge_1	2.89(1)	Er_2-1Ge_3	3.04(1)	Er_2-2Er_2	3.89(2)
$-2Ge_1$	2.91(1)	$-2Ge_2$	3.12(3)	$-2Er_2$	4.0526(1)
$-2Ge_3$	3.02(3)	$-1Er_1$	3.83(2)		
$-1Ge_3$	3.03(1)	$-1Er_1$	3.85(2)		
Ge_1-1Ge_2	2.53(1)	Ge_1-2Er_2	2.91(1)	Ge_1-1Ge_3	3.56(1)
$-1Ge_2$	2.56(1)	$-2Er_1$	3.283(3)	$-2Ge_3$	3.67(4)
$-2Er_2$	2.89(1)	$-1Ge_3$	3.53(1)	$-2Ge_1$	3.89(2)
Ge_2-1Ge_4	2.441(7)	Ge_2-2Er_1	2.94(3)	Ge_2-1Ge_4	3.41(1)
$-1Ge_1$	2.53(1)	$-2Er_1$	2.98(3)	$-1Ge_4$	3.81(1)
$-1Ge_1$	2.56(1)	$-2Er_2$	3.119(3)	$-2Ge_2$	3.89(2)
Ge_3-4Ge_3	2.81(1)	Ge_3-1Er_2	3.04(1)	Ge_3-2Ge_1	3.667(4)
$-2Er_2$	3.020(3)	$-1Ge_1$	3.54(1)	$-2Ge_3$	3.89(2)
$-1Er_2$	3.02(1)	$-1Ge_1$	3.56(1)		
Ge_4-2Ge_4	2.04(1)	Ge_4-2Er_1	2.97(2)	Ge_4-1Ge_2	3.81(1)
$-1Ge_2$	2.441(7)	$-2Er_1$	3.39(3)	$-2Ge_4$	3.89(1)
$-2Er_1$	2.927(7)	$-1Ge_2$	3.41(1)		

Acknowledgments

This work is financially supported by the Swiss National Foundation, Bern.

References

- [1] V.N. Eremenko and I.M. Obushenko, *Non-ferrous Metal Res.*, 9(3) (1981) 216.
- [2] J.V. Duboz, P.A. Badoz, A.Perie et al., *Appl. Surf. Sci.*, 38 (1989) 711.
- [3] F.P. Netzer, *J. Phys.: Condens. Matter*, 7 (1995) 991–1022.
- [4] J. Rodriguez-Carvajal, *Physica B*, 192 (1993) 55–69.
- [5] L.G. Akselrud, Yu.N. Grin, P.Yu. Zavalij, V.K. Pecharsky and V.S. Fundamensky, *Proc. XIIIth Europ. Crystallogr. Meeting, Moscow, August 1989*, VINITI, Moscow, 1989, p. 155.
- [6] I.R. Mokra, V.K. Pecharsky, Z.M. Shpyrka, O.I. Bodak, V.K. Belsky and I.E. Pats, *Dop. AN Ukr. SSR, Ser. B*, 3 (1989) 48.
- [7] P. Schobinger-Papamantellos, D.B. de Mooij and K.H.J. Buschow, *J. Less-Common Metals*, 163 (1992) 319.
- [8] O.Ya. Mruz, V.K. Pecharsky, O.I. Bodak and B.O. Bruskov, *Dop. AN Ukr. SSR, Ser. B*, 6 (1987) 51–53.
- [9] V.A. Koptzik, *Shubnikov Groups* (Moscow 1966).
- [10] W. Ospechowski and R. Guccione, in G.T. Rado and H. Suhl (eds.), *Magnetism IIA*, Academic Press, London, 1965, Ch 3, p. 105.
- [11] A.C.C. Wilson (ed.), *International Tables for Crystallography*, Vol. C, Kluwer Academic Publishers Dordrecht/Boston/London, 1992.
- [12] P. Schobinger-Papamantellos, D.B. de Mooij and K.H.J. Buschow, *J. Alloys Compounds*, 144 (1988) 265–274.
- [13] P. Schobinger-Papamantellos, J. Rodriguez-Carvajal, T. Janssen and K.H.J. Buschow, *Proc. Int. Conf. Aperiodic Crystals, Les Diablerets, Switzerland, 18–22 Sept., 1994*, p. 302.
- [14] P. Schobinger-Papamantellos, T. Janssen and K.H.J. Buschow, *J. Mag. Magn. Mat.*, 154 (1996) 29.
- [15] P. Schobinger-Papamantellos, G. Andre, J. Rodriguez-Carvajal, C.H. de Groot and K.H.J. Buschow, *J. Alloys Compounds*, 232 (1996)